Int. J. Electrochem. Sci., 12 **(2017)** 10023 – 10031, doi: 10.20964/2017.11.75

International Journal of
ELECTROCHEMICAL
SCIENCE
www.electrochemsci.org

Short Communication

Investigation of Morphological, Structural and Electrical Properties of Cds/ PMMA Nanocomposite Film Prepared by Solution Casting Method

Chan Kok Sheng[1,*], *Khairul Anuar Mat Amin*[1], *Loo Leong Hong*[2], *Mohd Faiz Hassan*[1], *Mohammad Ismail*[2]

[1] School of Fundamental Science, Universiti Malaysia Terengganu, 21030 UMT Kuala Terengganu, Terengganu, Malaysia
[2] School of Ocean Engineering, Universiti Malaysia Terengganu, 21030 UMT Kuala Terengganu, Terengganu, Malaysia
[*]E-mail: chankoksheng@umt.edu.my

Received: 7 August 2017 / *Accepted:* 18 september 2017 / *Published:* 12 October 2017

In this study, cadmium sulphide/ poly(methyl methacrylate) (CdS/PMMA) nanocomposite films with different content of CdS were prepared by a new solution casting method. The composite films were characterized by scanning electron microscopy (SEM), Fourier transform infrared spectroscopy (FTIR) and the conductivity was elucidated via electrochemical impedance spectroscopy (EIS). SEM revealed that CdS particle were homogeneously dispersed in PMMA polymer matrix, the size of CdS particles increased and became more agglomerated with the increasing of CdS. The Fourier transform infrared spectroscopy (FTIR) spectra indicated the presence of sulfur (S) in PMMA matrices at peak 841 cm^{-1}, meanwhile the intensity of absorption band in the range between (1790 – 1675) cm^{-1} and (1220 – 1095) cm^{-1} enhanced as the increase of CdS content. The EIS result showed that increasing quantity of CdS in PMMA matrix has resulted the increasing of electrical conductivity, which can be associated to the increased contact and Cd^{2+} ion transference between the CdS particles as evidenced by SEM images.

Keywords: poly(methyl methacrylate), cadmium sulphide, nanocomposite film, conductivity, morphology

1. INTRODUCTION

Cadmium sulphide, CdS is a II-VI semiconductor with band gap of 2.42 eV at room temperature and displays excellent optical and luminescent properties, such as the fluorescence and photoluminescence. According to Kozhevnikova et al. [1], microsized CdS particles used as

reinforcing agents scatter light, thus reducing light transmittance and optical clarity. Efficient particle dispersion combined with good polymer–particle interfacial adhesion eliminates scattering and allows the exciting possibility of developing strong yet transparent films, coatings and membranes. CdS also has a good sense to light where the conductivity increases when irradiated to light. This leading to be application as solar cell for photoelectric conversion, transistor for electronics switches and photodetector in infrared and visible region. CdS are hardly to be dispersed into chloroform or toluene due to their hydrophilic nature, however CdS can still be dispersed into ethanol and mixed with chloroform due to miscibility of ethanol with chloroform [2, 3].

Nanocomposites derived from nano-scale inorganic/organic particles that are dispersed in a polymer matrix homogeneously have attracted considerable attention. Organic/inorganic hybrid materials offer highly interesting and versatile applications when incorporated with a polymer. Among the inorganic/polymer nanocomposites, metal sulfides/polymer nanocomposites have been researched extensively due to their interesting optical, electrical and mechanical properties. Their excellent physical and chemical properties in various fields, such as catalysis, sensors, solar cells, photo detectors, light emitting diodes and laser communication, have made them very attractive and promising materials [4-6]. In recent years, it has been widely studied and synthesized the semiconductor particles with polymers to form the composite due to the enhancement of many physical properties such as optical and electrical properties for photoconductivity and photocatalyst applications [7]. CdS/polymer composite has attracted the interest of a number of researchers due to their synergistic and hybrid properties. Previously, CdS has been developed without a suitable support, it is undesirable since CdS aggregate due to the high surface energy, reducing surface area and restricting control over particle size. To overcome this problem, CdS have been composited with polymer**.** This makes CdS offer unique electrical and optical properties. Polymers also give an effective dispersion of CdS in the polymer matrix. CdS/polymer composite not only improved on properties of CdS but also offer a dramatic effect on mechanical properties of polymer where CdS used as filler in polymer matrix. Dixit et al. [8] reported the addition of CdS nanoparticle in PMMA gives the higher value of transition temperature due to their more rigid structure. Meanwhile, the polymer can serve as a protector and structure support for CdS from being scratched or other external phenomena that will affect the CdS initial structure. Furthermore, Due to the excellent optical properties of CdS, the polymer matrix used for this composite fabrication must be highly transparent which allows the photon to penetrate into the substrate and further received by CdS. The polymers that has such properties are like poly (methyl methacrylate) (PMMA) and polyvinyl alcohol (PVA) [7-11].

There are various methods have been employed to prepare the CdS/polymer composite by dispersing or embedding the CdS into the polymer matrix. Pedone et al. [12] has produced the composite by embedding the CdS nanoparticle into PMMA matrix using photocuring process, which is photoinduced hardening of a monomeric substrate. Rismana [13] had synthesized different-sized CdS nanoparticles inside various polymer matrices by direct miniemulsion polymerization and ion exchange technique. Conventionally, CdS and polymer were performed separately, and then CdS and polymer were mechanically mixed to form composite due to ease in preparation [8, 14]. However, sometimes it is difficult to disperse CdS into the polymer matrix homogeneously owing to the high viscosity of polymer. According to Rong et al. [10], CdS can be homogeneously dispersed in organic

solvents and polymer matrices by ultrasonic agitation to ensure an even arrangement. Thus in this study, we first investigate the surface morphology, structural bonding and electrical conductivity of CdS/PMMA nanocomposites prepared by a new solution casting method under ultrasonic agitation using ethanol and chloroform as solvents, and benzoyl peroxide as initiator to induce polymerization.

2. EXPERIMENTAL

2.1 Preparation of CdS/PMMA composite

CdS/PMMA composite films were prepared by a simple new solution casting method. In this method, PMMA (Sigma-Aldrich) was firstly dissolved in chloroform solvent with constant stirring for 2 hours using a magnetic stirrer. Simultaneously, the CdS nanopowder (Sigma-Aldrich) with different weight percentages (0 wt%, 5 wt%, 10 wt%, 20 wt%, 25 wt%) was added into ethanol to disperse CdS powder under constant stirring for 2 hours. Both PMMA and CdS solutions were then mixed together by adding the benzoyl peroxide for another half an hour of stirring. The mixtures were then dispersed in ultrasonic agitation for one hour to ensure CdS powder is uniformly dispersed in the solution. These homogeneous solutions were poured into flat-bottomed petri dish and dried at 75 ^{o}C in the oven to allow the solvent to evaporate. After five days, the CdS/PMMA composite films with different weight percentage were peeled off from the petri dish. The films were kept in desiccators for further drying before being characterized to ensure no water present in the present composite films.

2.2 Fourier transform infrared spectroscopy (FTIR)

The functional groups of CdS/PMMA composites were determined using the Thermo Ni-colet 380 FTIR spectrometer at room temperature. The spectrometer was equipped with an Attenuated Total Reflection (ATR) accessory with a germanium crystal. The sample was put on germanium crystal and infrared light was passed through the sample with the frequency ranging from 4000 - 550 cm^{-1} with scanning resolution of 16 cm^{-1}.

2.3 Scanning electron microscope (SEM)

The morphology of the composites and the distribution of the particles were characterized by using scanning electron microscope model JEOL JSM-6360LA at 15kV accelerating voltage. The samples were coated with a fine gold layer before obtaining the micrographs.

2.4 Electrochemical impedance spectroscopy (EIS)

The composite samples were cut into small discs of 2 cm diameter and sandwiched between two stainless steel electrodes under spring pressure. The samples were characterized via Electrical Impedance Spectroscopy (EIS) using HIOKI 3532-50 LCR Hi-Tester interfaced to a computer in a

frequency range from 42 Hz to 1 MHz. The measurements were performed at room temperature of 300 K until 308 K. The conductivity can be calculated from the equation

$$\sigma = t / R_b A \quad (1)$$

where A (cm^2) is the electrode-electrolyte contact area of the film and t is its thickness. R_b is bulk resistance obtained from the complex impedance plot (Cole–Cole plot) at the intersection of the plot and the real impedance axis.

3. RESULTS AND DISCUSSION

To generate the image of composite to high resolution, SEM is used to observe the particle size of the samples. Figure 1(a) presented the SEM images of pure PMMA. As we can see, the pure PMMA has a clear and smooth area of surface, which indicates transparent of PMMA. Figure 1(b)-(d) presented for CdS/PMMA composite samples with different wt% ratio of CdS in PMMA matrix.

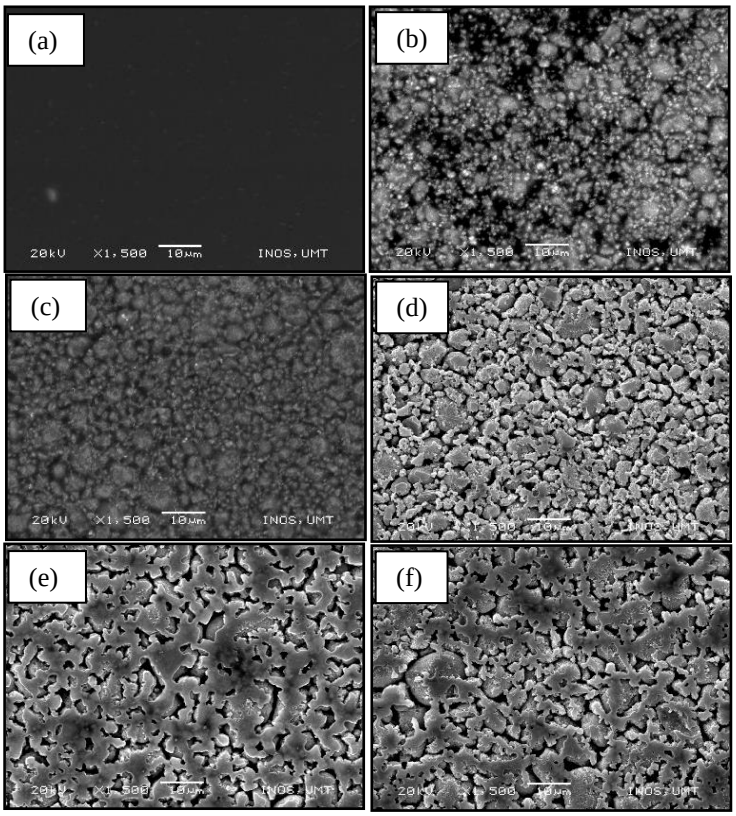

Figure 1. SEM micrograph **(X1500)** of (a) pure PMMA and PMMA/CdS composite with (a) 0wt %, (b) 5 wt %, (c) 10 wt% (d) 15 wt %, (e) 20 wt %, (f) 25 wt% of CdS.

From these images, it could be seen the CdS particles were homogeneously dispersed in the PMMA matrix. The average particle size of CdS in PMMA matrix is about (1.0-2.0) μm for 5 wt% of

CdS in PMMA matrices. When the content of CdS increases, the size of CdS particles increase and the CdS particles become agglomerated. This phenomenon indicates that highly amount of CdS can affect the agglomeration of CdS. As the particle size increases, the surface area will be decreased which lead to increasing of contact between the particles which also increasing the conductivity of CdS/PMMA composite. This is in agreement with Vishal and Sharma [15], which reported that CdS nanoparticles settle down at the void sites of PMMA matrix and form exfoliated nanocomposite, suggesting that the overall compatibility of the respective blend system increases with incorporation of CdS contents.

Figure 2 showed the FTIR spectra for the PMMA containing different weight percentage content of CdS. From the spectra, the double absorption peak observed at 2994 cm^{-1} and 2948 cm^{-1} represented the C-H stretching mode. The absorption peak observed at 1727 cm^{-1} is due to C=O asymmetric stretching of the carbonyl group. Other peaks observed at 1442 cm^{-1} and 1390 cm^{-1} were assigned to the O-CH_3 asymmetric bending and CH_2 twisting, while the absorption band located between (1260 – 1000) cm^{-1} indicated the C-O stretching [16-17].

There exist one characteristics peak in different assembly stage at 841 cm^{-1} which indicates the S-O stretching mode. From this result, it implied that there was the presence of sulfur in PMMA matrices. However, the Cd^{2+} was not detected in the spectra since the Cd-S bond is in the region lower than 500 cm^{-1}. Wang et al. [14] had reported that the vibrational absorption peak of Cd-S bond was located at 405 cm^{-1}, and Seoudi et al.[3] also reported that the main absorption band of CdS at 260 cm^{-1} could be assigned to the Cd-S stretching vibration. Meanwhile, the peaks occurred within the range of (1790 – 1675) cm^{-1} and (1220 – 1095) cm^{-1} showed increase in the intensity of absorption with the increase of CdS. This showed that the C=O bond at 1790 - 1675 cm^{-1} and C-O bond at 1220 – 1095 cm^{-1} have promoted the change of dipole moment in molecular vibration with the increase in wt % of CdS [16-18].

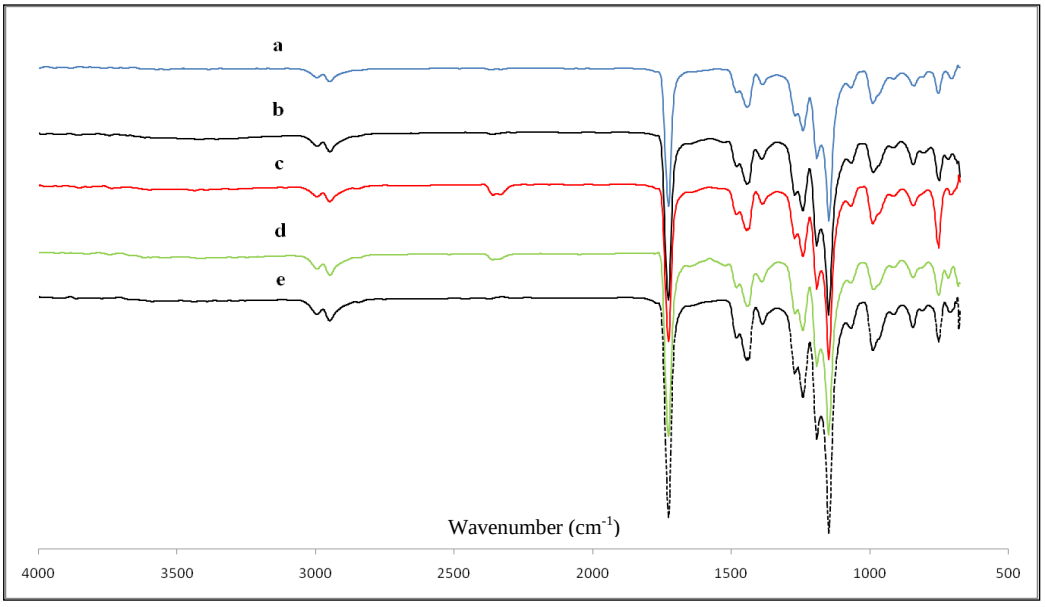

Figure 2. FTIR spectra of (a) pure PMMA and PMMA/CdS composite with (a) 0wt %, (b) 5 wt %, (c) 10 wt% (d) 15 wt %, (e) 20 wt %, (f) 25 wt% of CdS.

The electrical conductivity of CdS/PMMA composite films were obtained from the Cole-Cole plot of EIS spectra for CdS/PMMA composite films formulated at different composition of CdS as shown in Figure 3 (a) – (f). The x-axis represented the series equivalent resistance and y-axis represented the reactance. From Figure 3(a) – (e), their impedance spectra were scattered and causing a difficulty to obtain the bulk resistance R_b except for Figure 3(f) which showing a semicircle curve. This could be due to the unstable of Cd^{2+} ion of mobile charge carrier distributed in PMMA matrix. In order to obtain the bulk resistance R_b, a semicircle was drawn on the impedance spectra closest to the best fitting on scattered point.

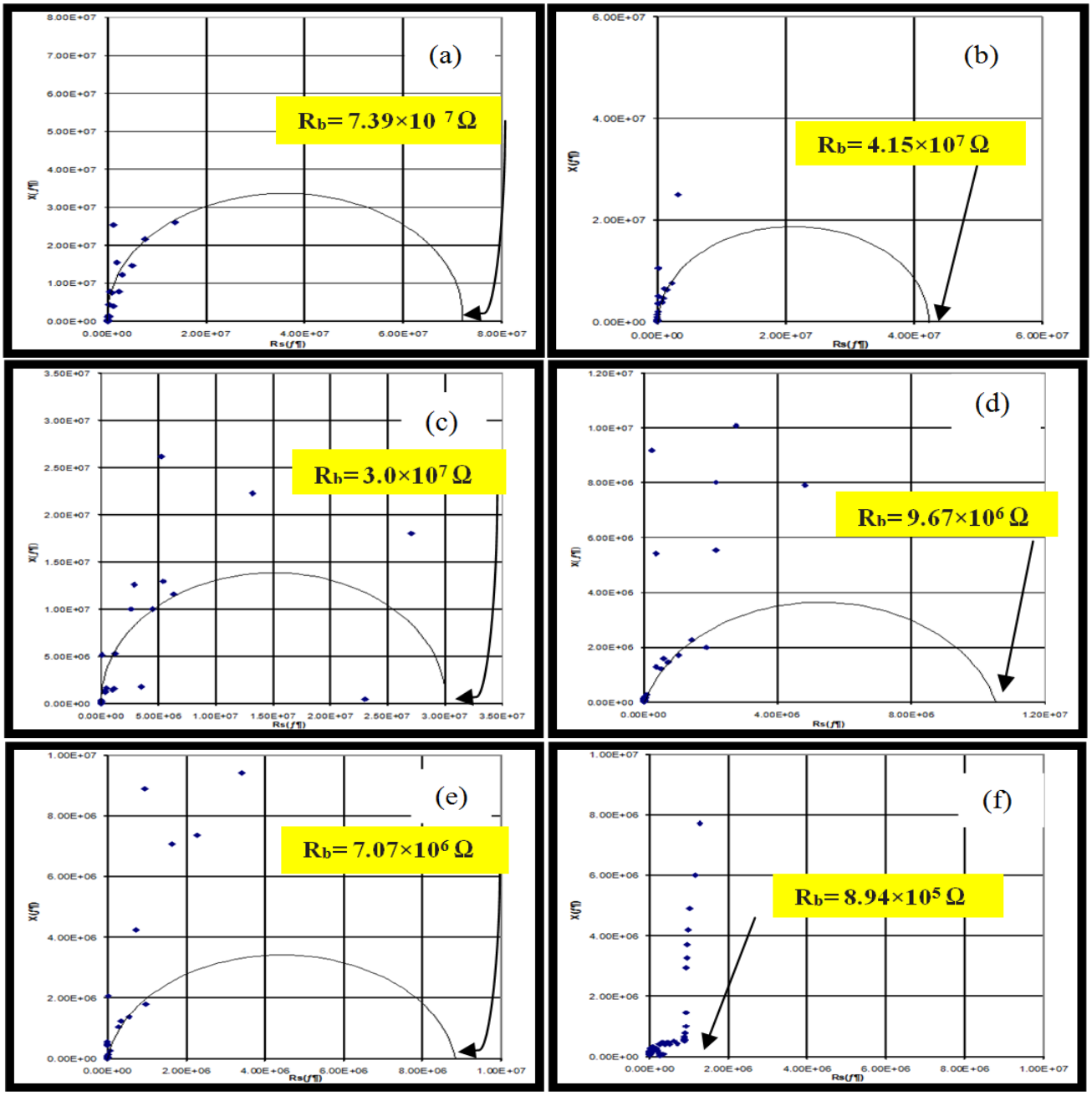

Figure 3. EIS spectra of (a) pure PMMA and PMMA/CdS composite with (a) 0wt %, (b) 5 wt %, (c) 10 wt% (d) 15 wt %, (e) 20 wt %, (f) 25 wt% of CdS.

The bulk resistance will then be obtained at right end of semicircle. From Fig. 3(f), it could see that the Cole-Cole plot showing the semicircle curve. This showed that the composite with 25 wt% of CdS in PMMA has achieved a stable Cd^{2+} ion of mobile charge carrier in PMMA matrix. The R_b values were calculated using equation (1) in order to obtain the conductivity of CdS/PMMA composite. Table 1 tabulated all the parameter values of bulk resistance R_b, thickness of sample and the conductivity σ in different composition of CdS. The bulk resistance decreased with the increase of wt % of CdS.

Table 1. Bulk resistance, sample thickness and electrical conductivity of CdS/PMMA composite with different content of CdS.

CdS content (wt %)	Bulk resistance, R_b (Ω)	Thickness, t (cm)	Conductivity, σ (Scm^{-1})
0	7.39×10^{7}	0.004	1.72×10^{-11}
5	4.15×10^{7}	0.004	3.07×10^{-11}
10	3.0×10^{7}	0.016	1.70×10^{-10}
15	9.67×10^{6}	0.007	2.30×10^{-10}
20	7.07×10^{6}	0.017	7.65×10^{-10}
25	8.94×10^{5}	0.008	2.85×10^{-9}

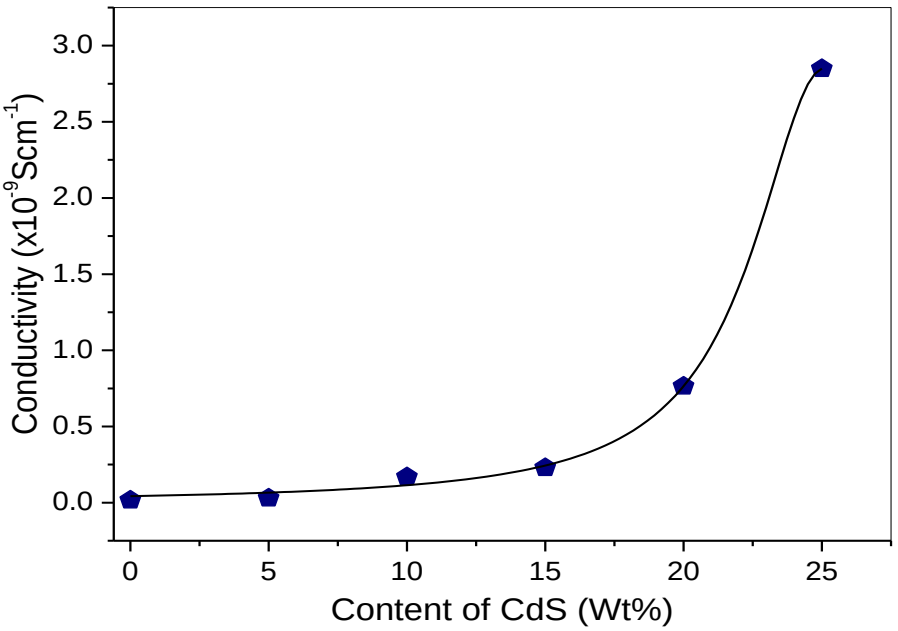

Figure 4. Conductivity against CdS content for CdS/PMMA composites.

The conductivity of CdS/PMMA composite was plotted against wt % of CdS as shown in Figure 4. The conductivity values were lying in the range between (1.72×10^{-11} - 2.85×10^{-9}) Scm^{-1}**.** From the figure, the values of the electrical conductivity for the composites are higher than that of pure PMMA. This refers to the facilitating of the conduction process through the presence of quantum dots, which either lie in the energy gap or act as donor and acceptor sites. These sites facilitate the hopping

of electrons between valence and conduction bands and hence increasing the dc electrical conductivity [18, 19].

Also, the conductivity increased gradually from ~10^{-11} Scm^{-1} to ~10^{-9} Scm^{-1} with the increasing of CdS content from 5 wt% to 15 wt%. The increase in conductivity could be attributed to increase the number of mobile charge carriers. This result is similar to the one reported by Al-Hosiny et al. [18], which indicates an efficient incorporation of quantum dots inside the polymer matrix and a strong interaction between PMMA and quantum dots. Subsequently, the conductivity increased rapidly from 15 wt % of CdS content due to the agglomeration of CdS in the matrix. This effect has already been evidenced by SEM morphological images. The drastic increase in the conductivity could be attributed to the increasing contact between the CdS particles and hence facilitating the transference of mobile charge carriers across the film [11-13].

4. CONCLUSION

A series of CdS/PMMA nanocomposite films were successfully prepared via solution casting method. SEM images showed that the CdS particle were homogeneously dispersed in PMMA matrix, the size of CdS particles increased and CdS particles become agglomerated at higher CdS content. FTIR indicated the presence of sulfur bonding in the composite at peak 841cm^{-1} and the absorption bonds intensity increases at the range of (1790 – 1675) cm^{-1} and (1220 – 1095) cm^{-1} with the increasing of CdS wt%. Meanwhile, the increasing of CdS content has resulted in increasing the conductivity, which can be associated with increase contact between CdS particles caused by agglomeration as evidenced by SEM micrograph.

ACKNOWLEDGEMENT
The authors would like to thank School of Fundamental Science, School of Ocean Engineering, Universiti Malaysia Terengganu and research grant (FRGS-59140) by Malaysian Government for the helps and financial support of this work.

References

1. N. S.Kozhevnikova., A. A. Rempel, F. Hergert and A. Magerl, *Russ. J. Phys. Chem*., 81(2005) 768.
2. B. Pradhan, A. K. Sharma and A. K. Ray, *J. Cryst. Growth*, 304 (2007) 388.
3. R. Seoudi, A. Shabaka, W. H. Eisa, B. Anies and N. M. Farage, *Physica B*, 405 (2009): 919.
4. Z. M. Johannes and A. A.Peter, *Polymers*, 6 (2014) 2322.
5. T. P. Mthethwa, M. J. Moloto, A. de Vries and K. P. Matabola, *Mater. Res. Bull*., 46 (2011) 569.
6. M. Ranjbar, M. Yousefi, R. Nozari and S. Sheshmani, *Int. J. Nanosci. Nanotechnol.*, 9(2013) 203.
7. P. Rodriguez, A. N. Munoz, M. E. San-Martin, C. G. Gonza´lez, S. A. Tomas and A. O. Zelaya, *J. Cryst. Growth*, 310 (2008) 160.
8. M. Dixit, S. Gupta, V. Mathur, K. S.Rathore, K. Sharma and N. S. Saxena, *Chalcogenide Lett*., 6 (2009)131.
9. P. K. Khanna and R. R. Gokhale, *Mater. Chem. & Phys*., 94 (2001) 454.
10. M. Z. Rong, M. Q. Zhang, H. C. Liang and H. M. Zeng, *Appl. Surf. Sci*., 228 (2004) 176.

11. S. Gudrun and M. M. Matthew, *Curr. Opin. Colloid Interface Sci*., 8 (2003)103.
12. L. Pedone, E. Caponetti, M. Leone, V. Militello, V. Panto, S. Polizzi and M. L. Saladino, *J. Colloid and Interface Sci*., 284 (2005) 495.
13. Rismana. (2010), Thesis of Doctor of Philosophy, Universiti Teknologi Malaysia.
14. H. M. Wang, P. F. Fang, Z. Chen and S. J. Wang, *Appl. Surf. Sci*., 253 (2007) 8495.
15. M. Vishal and K. Sharma, *Adv. in Nanoparti*., 2 (2013) 205.
16. Thermo Nicolet. Introduction to Fourier Transform Infrared Spectrometry. http://mmrc.caltech.edu/FTIR/FTIRintro.pdf. [Access online 20 January 2010].
17. Walt Volland (1999). Organic Compound Identification Using Infrared Spectroscopy. http://www.800mainstreet.com/irsp/eir.html. [Access online 4 March 2010].
18. N. M. Al-Hosiny, S. Abdallah, M. A. A. Moussa and A. Badavi, *J. Polym. Res.*, 20 (2013) 76.
19. F. Yakuphanoglua,I. S. Yahia, G. Barim and B. FilizSenkal, *Synth. Metals*, 160 (2010) 1718.